Low-temperature magnetoresistance of individual single-walled carbon nanotubes: A numerical study

Zhenhua Zhang*
Department of Information and Calculating Science, Changsha Communications College, Changsha 410076, The People's Republic of China
and Department of Applied Physics, Hunan University, Changsha 410082, The People's Republic of China

Jingcui Peng and Xiaoyi Huang
Department of Applied Physics, Hunan University, Changsha 410082, The People's Republic of China

Hua Zhang
Department of Information and Calculating Science, Changsha Communications College, Changsha 410076, The People's Republic of China

(Received 25 July 2001; revised manuscript received 17 December 2001; published 5 August 2002)

The low-temperature magnetoresistance induced by an axial magnetic field in individual single-walled carbon nanotubes (SWNTs) is studied numerically based on Boltzmann transport equation and π electronic energy dispersion relations for individual SWNTs as well as taking one-dimensional weak localization (WL) into account. It is shown that the Altshuler-Aronov-Spivak effect related to WL is much weaker in individual SWNTs than in individual multiwalled carbon nanotubes, whereas the Aharonov-Bohm (AB) effect related to tubular energy band structure is stronger in individual SWNTs when the conducting electrons occupy lower energy levels, but this effect weakens rapidly as conducting electron energy increases. This suggests that only the AB effect can be observed remarkably in the states of the conducting electrons with lower energy.

DOI: 10.1103/PhysRevB.66.085405 PACS number(s): 72.15.Gd, 73.61.Wp, 73.50.−h

I. INTRODUCTION

Recently, the research of the carbon nanotubes (CNs), narrow seamless graphene cylinders with nanometer-size diameter and micrometer-size length as constituents of nanoscale material and structure, has attracted much attention. They are expected to have unprecedented potential practical applications in nanoelectronics for developing nanoelectronic devices. Individual single-walled carbon nanotubes (SWNTs) can be applied as conducting quantum wires,[1,2] field-effect transistors,[3] single-electron tunneling transistors,[1,2] and spin-electronic devices.[4] Combination of nanotubes can be used as rectifiers[5] or more complex multiterminal devices.[6] However, for rational design of these devices, a fundamental understanding of the electrical and magnetic properties of CNs and how they depend on their structural parameters such as the diameter, number of concentric shells, and chirality of tubes, etc., is required.

An important method to describe the electronic transport behaviors involves directly measuring the magnetoresistance of CNs defined as $\Delta\rho/\rho(0)[\Delta\rho=\rho(B)-\rho(0)]$. Recently, an advanced technique for magnetoresistance measurements in CNs has already been used to investigate the transport mechanism.[7–12] The transverse magnetoresistance (when the applied magnetic field is perpendicular to the tubular axis) has been measured for graphite nanotube bundles,[7] multiwalled CNs (MWNTs),[8] an oriented CN film,[9] an entangled SWNT network[10] and a ring of SWNTs (Ref. 11) (strictly speaking, a ring consisting of a SWNT bundle), and an intercalated CN bundle.[12] The measured negative magnetoresistance has been described consistently within the framework of the weak localization (WL) theory.[13] WL originates from the quantum-mechanical treatment of the backscattered partial electron waves traveling back to the original point along the time-reversed path, which contains an interference term adding up constructively. Enhanced backscattering, thereby, causes a resistance increasing and it is larger than the classical Drude one, while the interference term is canceled in a magnetic field of sufficient strength, hence a negative magnetoresistance is observed. When the applied magnetic field is parallel to the tube axis, periodic oscillations of magnetoresistance with period $\Phi_0/2$ or Φ_0 (where $\Phi_0 \equiv h/e$ is the magnetic flux quantum) have been observed and reported for individual MWNTs, Bachtold *et al.*[14] ascribed the phenomenon having period of magnetic flux $\Phi=\Phi_0/2$ to the Altshuler-Aronov-Spivak (AAS) effect.[15] Fujiwara and Tomiyama[16] attributed the phenomenon of period taking $\Phi=\Phi_0$ to the Aharonov-Bohm (AB) effect.[17] Here, the AAS effect originates from the quantum interference between partial electronic waves encircling a tube and traveling back to the original point in opposite direction,[14] whereas the AB effect arises from the dependence of the electron wave function on the vector potential[17] causing the phase shift of the electron wave function and hence strongly affecting the band structure of SWNTs.[18–20]

As we know, up to now, the experimental data or theoretical calculations for magnetoresistance properties of individual SWNTs have not been reported. Considerable difficulties are encountered in experimentally measuring the magnetoresistance of individual SWNTs. Generally speaking, individual SWNTs are less rigid in the direction perpendicular to the tubular axis so that they are susceptible to spontaneous deformation. Furthermore, SWNTs are easily bent by the tip of atomic force microscope or crossing over

electrodes induce a radial deformation that flattens the tubes[21,22] and influences their electronic properties. Therefore, it is significant to calculate the magnetoresistance of individual SWNTs in order to predict the measurement results in the ideal case.

In this paper, we assume the applied magnetic field to be parallel to the tube axis of individual SWNTs, and both AAS and AB magnetic quantum effects, which are related to WL and band structure, respectively, are considered together. A theoretical model is proposed for calculating the magnetoresistance of individual SWNTs within the framework of dispersion relations of π electronic energy for individual SWNTs in magnetic field and Boltzmann transport equation and WL theory.

II. THEORETICAL MODEL

First, we consider the magnetoresistance induced by a parallel magnetic field and influenced by the effect of WL. The contribution of WL to magnetoresistance can be ascribed to change of the phase-coherence length L_φ in magnetic field. This is because one-dimension (1D) WL correction ΔG to the conductance G can be expressed as $-0.62e^2L_\varphi/\hbar L$,[23] where L is the length of the tube. The inclusion of magnetic field parallel to the axis of the tube results in the phase-coherence length L_φ becoming field dependent,[23,24]

$$\frac{1}{L_\varphi^2(B)}=\frac{1}{L_\varphi^2(0)}+\frac{w^2}{3l_m^4}, \tag{1}$$

where w is the wall thickness of cylindrical system and l_m is the magnetic length defined by $l_m^2=\hbar/eB$. We have noted that $L_\varphi(0)$ and $\sqrt{3}l_m^2/w$, for MWNTs and rings of SWNTs in weak magnetic flux, are of the same order of magnitude ($\sim$1 nm).[11,23] As for the ideal case of a long SWNT, its $L_\varphi(0)$ is roughly of the same order of magnitude as that of MWNTs and the ring of SWNTs,[11,23,25,26] but its wall thickness w is of the same order of magnitude as the diameter of a carbon atom and much less than the wall thicknesses of both MWNTs and the ring of SWNTs. In general, $3l_m^4/w^2$ is two orders higher than $L_\varphi^2(0)$ (for given l_m). It implies that the AAS effect related to WL in a SWNT is much weaker than in a MWNT or in a ring of CNs. Therefore, for simplicity, we will not directly take the AAS effect into account in the following numerical calculation and only take it as a comparative reference to the AB effect.

A uniform magnetic field $\boldsymbol{B}$ applied along the axis of a SWNT leads to vector potential $\boldsymbol{A}$ having the circumferential direction[19] and constant magnitude of $A=B\cdot R/2$ on the surface of the cylinder. When an electron travels along the circumference, the additional phase shift of the electron wave function due to deviating x from origin point O is[27]

$$\gamma=\frac{e}{\hbar}\int_0^x \boldsymbol{A}\cdot d\boldsymbol{L}=\frac{\Phi}{\Phi_0 R}x. \tag{2}$$

Using the periodic boundary condition $\Psi(\boldsymbol{r}+\boldsymbol{C_x})=\Psi(\boldsymbol{r})$, where $\Psi(\boldsymbol{r})$ is the electron's Bloch function, $\boldsymbol{C_x}=m\boldsymbol{a_1}+n\boldsymbol{a_2}$ is a chiral vector with $|\boldsymbol{C_x}|=2\pi R$, $\boldsymbol{a_1}$ and $\boldsymbol{a_2}$ are the primitive lattice vectors of the graphite sheet[28] with $|\boldsymbol{a_1}|=|\boldsymbol{a_2}|=a=2.46$ Å, the obtained transverse wave vector is

$$k_x=2\pi(p+\Phi/\Phi_0)/a\sqrt{(n^2+m^2+nm)}\quad (p=1,2,...,N),$$

where[29]

$$N=\frac{2(n^2+m^2+nm)}{d}\quad \text{if } n-m \text{ is not a multiple of } 3d$$

$$=\frac{2(n^2+m^2+nm)}{3d}\quad \text{if } n-m \text{ is a multiple of } 3d, \tag{3}$$

where d denotes the highest common divisor of integers m and n. For simplicity, we consider only the π subbands and neglect the effects caused by the finite tube curvature such as the mixture of σ and π bands and the interaction between p_z orbitals, and any Peierls distortions and the spin-B interaction (discussed below) are neglected too. The energy dispersion relations for a SWNT can be obtained within the framework of tight-binding calculation[19,30]

$$E^{(p)}(k_y\Phi)=\pm\gamma_0\left\{1+4\cos\left[\frac{\sqrt{3}a}{2}(k_y\cos\theta+k_x\sin\theta)\right]\times\cos\left[\frac{a}{2}(k_y\sin\theta-k_x\cos\theta)\right]+4\cos^2\left[\frac{a}{2}(k_y\sin\theta-k_x\cos\theta)\right]\right\}^{1/2}, \tag{4}$$

where $\gamma_0=2.66$ eV is the transfer integral for the nearest-neighbor interaction, $\cos\theta=(2m+n)/2\sqrt{m^2+n^2+mn}$, $\sin\theta=\sqrt{3}n/2\sqrt{n^2+m^2+nm}$, and chiral angle θ is the angle included between the vectors $\boldsymbol{C_x}$ and the "zigzag" edge with values $0°\leqslant\theta\leqslant30°$. Obviously, the energy dispersion relations in Eq. (4) is periodic because of Φ with period Φ_0 due to the AB effect.

The Boltzmann transport equation has been applied successfully to study the electronic transport properties of SWNTs.[25,26,31–33] In our previous work,[26] evaluated low-temperature resistance of individual SWNTs based on the Boltzmann transport equation are in good agreement with the experimental data. For a homogeneous medium with uniform temperature, lying in an uniform magnetic field $\boldsymbol{B}$ and electric field $\boldsymbol{\varepsilon}$, the Boltzmann equation under relaxation time τ approximation can be expressed as

$$f=f_0+\frac{e\tau}{\hbar}(\boldsymbol{\varepsilon}+\boldsymbol{u}\times\boldsymbol{B})\cdot\boldsymbol{\nabla}_k f, \tag{5}$$

where f is the electronic distribution function of nonequilibrium configuration, f_0 is the Fermi distribution function, and $\boldsymbol{u}=(1/\hbar)\boldsymbol{\nabla}_k E$ is the band velocity, assuming

$$f=f_0+\frac{\partial f_0}{\partial E}\varphi, \tag{6}$$

where φ is defined as a small quantity. Substituting Eq. (6) into Eq. (5) under high-order approximation, we obtain

$$\varphi=\left\{\frac{e\tau}{\hbar}\boldsymbol{\varepsilon}\cdot\boldsymbol{\nabla}_k E+\frac{e^2\tau^2}{\hbar m^*}(\boldsymbol{B}\times\boldsymbol{\varepsilon})\cdot\boldsymbol{\nabla}_k E + \frac{e^3\tau^3}{\hbar m^{*2}}\boldsymbol{B}\times(\boldsymbol{B}\times\boldsymbol{\varepsilon})\cdot\boldsymbol{\nabla}_k E\right\}, \quad (7)$$

thus, Eq. (6) can be rewritten as

$$f=f_0+\frac{\partial f_0}{\partial E}\left\{\frac{e\tau}{\hbar}\boldsymbol{\varepsilon}\cdot\boldsymbol{\nabla}_k E+\frac{e^2\tau^2}{\hbar m^*}(\boldsymbol{B}\times\boldsymbol{\varepsilon})\cdot\boldsymbol{\nabla}_k E + \frac{e^3\tau^3}{\hbar m^{*2}}\boldsymbol{B}\times(\boldsymbol{B}\times\boldsymbol{\varepsilon})\cdot\boldsymbol{\nabla}_k E\right\}. \quad (8)$$

As mentioned above, magnetic field $\boldsymbol{B}$ is parallel to the axis of a SWNT. When voltage V is applied to two ends of a SWNT, we take $\varepsilon=V/L$ and neglect the chiral effects, based on the assumption that the directions of electric field $\boldsymbol{\varepsilon}$, the band velocity $\boldsymbol{u}$, and the current I are all along the tube axis in the same direction as that of the magnetic field $\boldsymbol{B}$. For 1D-SWNTs, the magnetoconductance $G(\Phi)$ can be derived from Eq. (8) as follows:

$$G(\Phi)=\frac{e^2}{\pi\hbar^2 L}\sum_{p=1}^{M}\int_{\mathrm{FBZ}}\tau\left|\frac{\partial E^{(p)}(k_y,\Phi)}{\partial k_y}\right|^2 \times\left(-\frac{\partial f_0}{\partial E^{(p)}(k_y,\Phi)}\right)dk_y, \quad (9)$$

where $E^{(p)}(k_y,\Phi)$ is the dispersion relation of π electronic energy for a SWNT, FBZ represents the first Brillouin zone, and M is the number of channels for electronic transport. Assuming the temperature to be low enough so that $[-\partial f_0/\partial E^{(p)}(k_y,\Phi)]$ can be replaced by $\delta(E^{(p)}(k_y,\Phi)-E_F)$, we let $\tau=\tau(E_F)$ (E_F is the Fermi level) which is independent of the temperature and the energy levels.

According to the rigid-band model,[19] the Fermi level $E_F(0)$ without $\boldsymbol{B}$ field is determined by the free-carrier number per unit length, thus the doped SWNTs (or SWNTs with impurities) cause $E_F(0)$ shifting. When Φ varies, the free carriers will redistribute themselves among the different conduction subbands according to the variation of energy dispersions with Φ. The Fermi level also varies with Φ to keep the number of particles constant, but $E_F(\Phi)/E_F(0)\sim 1$[19]. k_F is the Fermi wave vector dependent on Φ. Similar to the aforementioned result, we may take approximately $\boldsymbol{k_F}(\Phi)\approx\boldsymbol{k_F}(0)=4\pi(\boldsymbol{a_1}-\boldsymbol{a_2})/3a^2$.[34]

III. NUMERICAL CALCULATION RESULTS AND DISCUSSION

In order to obtain relations of magnetoresistance vs magnetic flux Φ, the determination of the number of conduction channels (subbands) M is the key for the numerical calculation of magnetoresistance. Conducting electrons with different energy E caused by the varying electric field strength ε and heat excitation enter different channels (i.e., occupy different subbands), while the subbands continuously shift position in k space with changed magnetic flux Φ. It is clear that the number of conduction channels M is the function of electron energy E and magnetic flux Φ, i.e., $M=M(E,\Phi)$. We can deduce that SWNTs with $2m+n=3\times$integer ($\neq 3\times$integer) are metals (semiconductors) while $\Phi=0$ From Eq. (4). We take SWNT (15,0), (14,0), (9,9), and (12,6) having nearly the same radii as examples and using Eq. (9) to perform numerical calculation to obtain relations of magnetoresistance vs Φ at various conducting electron energy E. The energy of the spin-B interaction is $E(\sigma,\Phi)=\hbar^2 g\sigma\Phi/m^*R^2\Phi_0$, where g factor is taken to be the same as that (≈ 2) of the pure graphite, $\sigma=\pm\frac{1}{2}$ is the electron spin and m^* is the bare electron mass. In the case of our selected tubes ($R\sim 1$ nm), we have $E(\sigma)\sim 10^{-2}\Phi/\Phi_0$ (eV), therefore, in the range of weak magnetic flux ($\Phi\sim\Phi_0$), the Zeeman splitting could be neglected as compared with the subband level interval (~ 0.5 eV).

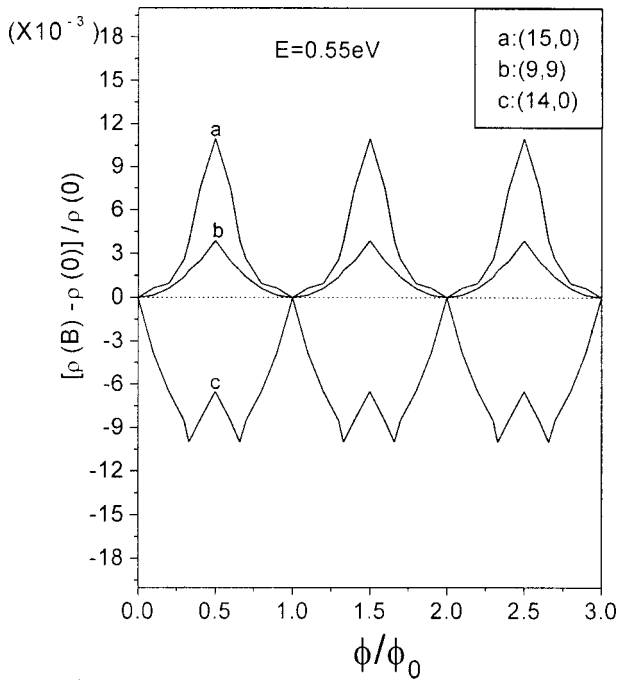

FIG. 1. The calculation results of low-temperature magnetoresistance for SWNT (15,0), (9,9), and (14,0) vs Φ in the states of conducting electrons with maximum energy $E_M=0.55$ eV. All results show that the dependence of magnetoresistance on Φ is consistent with energy gap $E_g(\Phi)$ dependent on Φ.

(1) Conducting electrons in weaker electric field (i.e., with lower energy). Figure 1 shows the calculated results for magnetoresistance vs Φ for SWNT (15,0), (14,0), and (9,9) in the states of electronic transport with maximum energy $E_M=0.55$ eV, which is near to the Fermi level, thus the electrons occupy lowest conduction subband, all of their magnetoresistances have the same oscillation period Φ_0. For metallic SWNT (15,0) and (9,9), positive magnetoresistances increase monotonically with increase in the magnetic field $\boldsymbol{B}$, and reach their maximum values at $\Phi=(\text{integer}+1/2)\Phi_0$, then they decrease gradually and become zero at $\Phi=\text{integer}\times\Phi_0$, whereas the semiconducting SWNT (14,0) always shows negative magnetoresistance, the minimum values of magnetoresistance occur at $\Phi=(\text{integer}+1/3)\Phi_0$.

The above results originate from the lowest unoccupied

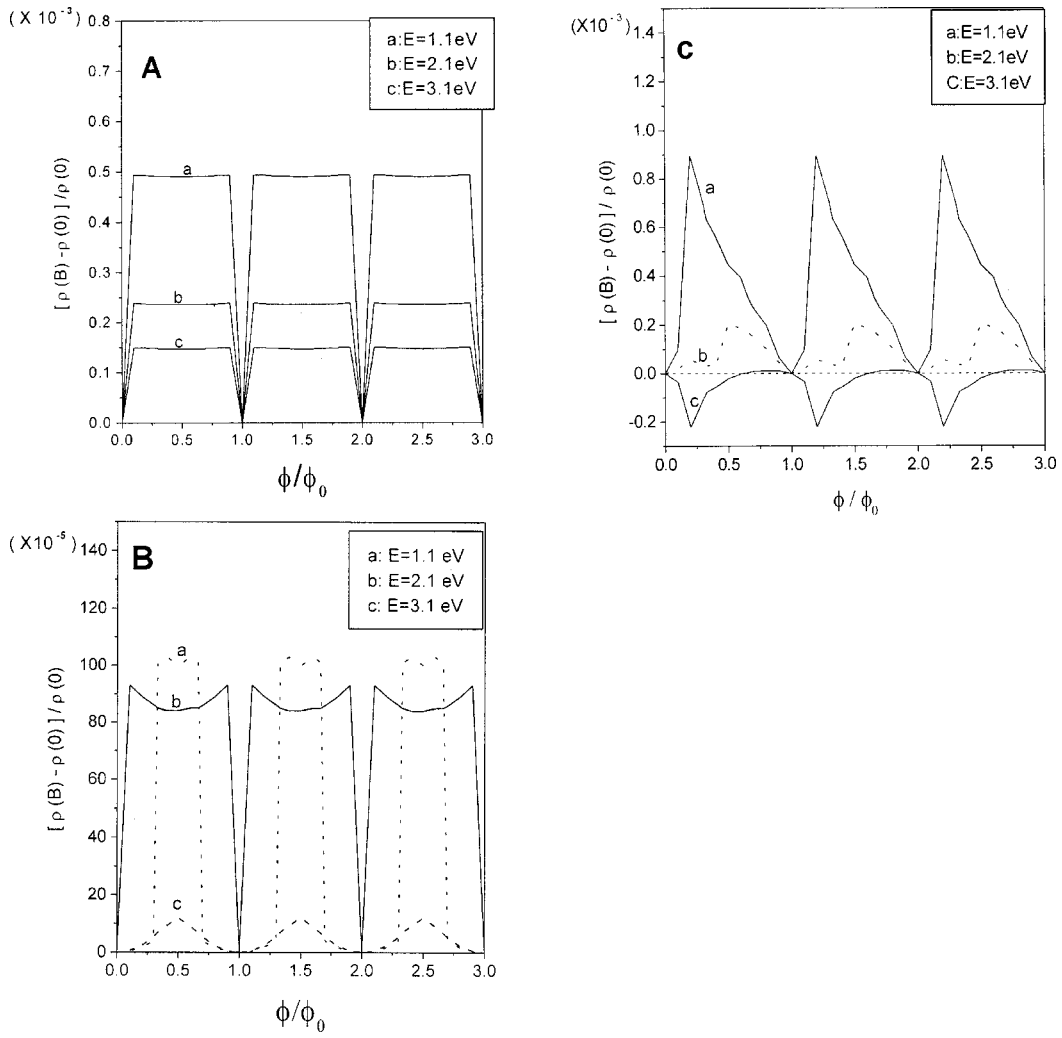

FIG. 2. The calculation results of low-temperature magnetoresistances of three SWNTs vs Φ: (A) for metallic armchair SWNT (9,9), (B) for zigzag SWNT (15,0), (C) for chiral SWNT (12,6), the curves of (a), (b), and (c) correspond to the conducting electrons with different maximum energy $E_M = 1.1$, 2.1, and 3.1 eV, respectively. All results show that the magnetoresistances decreases rapidly with increase in the energy of conducting electrons.

molecular orbital and the highest occupied molecular orbital in the proximity of Fermi level which is touched or untouchable by these subbands dependent on Φ with period Φ_0. Generally speaking, if radii R of SWNTs are large enough, $\sqrt{3}a \sin\theta/2R$ and $a \cos\theta/2R$ might be neglected. Thus from Eq. (4), we can deduce the energy gap expressions defined as $E_g(\Phi) = 2 \min\{|E(J,k_y\Phi)|\}$.

For chiral metallic SWNTs, the Φ-dependent energy gap $E_g(\Phi)$ is given as follows:

$$E_g(\Phi) = \begin{cases} \dfrac{\sqrt{3}\gamma_0 a \cos\theta}{R}\dfrac{\Phi}{\Phi_0} & \left(0 \leqslant \Phi \leqslant \dfrac{\Phi_0}{2}\right) \\ \dfrac{\sqrt{3}\gamma_0 a \cos\theta}{R}\left|1 - \dfrac{\Phi}{\Phi_0}\right| & \left(\dfrac{\Phi_0}{2} \leqslant \Phi \leqslant \Phi_0\right) \end{cases}. \tag{10}$$

For chiral semiconducting SWNTs, the Φ-dependent energy gap $E_g(\Phi)$ is given as

$$E_g(\Phi) = \begin{cases} \dfrac{\sqrt{3}\gamma_0 a \cos\theta}{R}\left|\dfrac{1}{3} - \dfrac{\Phi}{\Phi_0}\right| & \left(0 \leqslant \Phi \leqslant \dfrac{\Phi_0}{2}\right) \\ \dfrac{\sqrt{3}\gamma_0 a \cos\theta}{R}\left|\dfrac{2}{3} - \dfrac{\Phi}{\Phi_0}\right| & \left(\dfrac{\Phi_0}{2} \leqslant \Phi \leqslant \Phi_0\right) \end{cases}, \tag{11}$$

the $\cos\theta$ and R in $E_g(\Phi)$ expressions in Eq. (10) and Eq. (11) show that the chirality effect and the tubular radial size influence the energy gap. Obviously, the oscillations of calculated magnetoresistances in Fig. 1 are in good agreement with that of energy gap $E_g(\Phi)$ expressed in Eq. (10) and Eq. (11). Here, we would like to point out that $\cos\theta \approx 1$ because θ takes the values in the range as stated above, it suggests that $E_g(\Phi)$ varies only with Φ and geometric parameter R, which is consistent with the result of Ref. 20.

(2) Conducting electrons in stronger electric field (i.e., with higher energy). Figures 2(A), 2(B), and 2(C), respectively, show the calculated magnetoresistance for SWNTs

(9,9), (15,0), and (12,6). The curves of (a), (b), and (c) correspond to the conducting electrons with different maximum energy $E_M = 1.1$, 2.1, and 3.1 eV, respectively, which are far from the Fermi level with different distances. Electrons occupy more conduction subbands including one subband nearest to the Fermi level in the case of Fig. 1. Consequently, there are more complicated cases contributing to total magnetoresistance because of the involved channels having different band velocity ν and transport capability. The periods of the oscillations of magnetoresistance are still Φ_0, but the values of magnetoresistance are not dominated solely by the subband nearest to Fermi level so that the changing properties of energy gap $E_g(\Phi)$ [expressed in Eqs. (10) and (11)] are covered. The more interesting results as shown in Figs. 2(A), 2(B), and 2(C) are that magnetoresistance decreases rapidly with increase in the energy of conducting electrons. It implies that the AB effect almost vanishes when the conducting electrons occupy higher energy levels.

The magnetoresistance for individual SWNTs is the superposition of two components: the AB effect and the AAS effect (always having negative magnetoresistance) contribution. When the results in this section are compared with the weak AAS effect stated in Sec. II, we can draw a reasonable conclusion that for low-energy electron transport, the AB effect is the dominant factor resulting in the weak AAS effect being covered so that the AB effect can be observed remarkably, and for conducting electrons with higher energy, the AAS effect becomes dominant although its magnitude is still small, but the AB effect is still much weaker and almost vanishes.

If the above analysis is extended to MWNTs, the inconsistent experimental results observed by Fujiwara[16] and Bathtold,[14] respectively, can be explained naturally. The AAS effect is stronger in MWNTs than in SWNTs, therefore, the AB effect (the AAS effect) corresponds to the conducting electrons with lower (higher) energy so that both effects can be observed under the different conditions. It is reasonable to conclude that the conducting electrons occupying different levels leads to different effect (AB effect or AAS effect) being observed in different experiments for MWNTs.

IV. CONCLUSION

We present the calculated results for magnetoresistance induced by an axial magnetic field in individual SWNTs using the Boltzmann transport equation, in combination with the dispersion relations of π electronic energy and the theory of weak localization. The conditions of exhibiting the AAS effect on the AB effect are found out. The AAS effect in individual SWNTs is much weaker than that in individual MWNTs and the AB effect is much stronger in individual SWNTs as long as the conducting electrons occupy lower energy levels, therefore the AB effect is predicted to be significant in individual SWNTs. On the other hand, when the conducting electrons occupy higher energy levels in individual SWNTs, the AB effect almost vanishes and the AAS effect becomes dominant although its magnitude is still small. In other words, the exhibition of the AB effect or the very weak AAS effect should be associated with the energy of conducting electrons in individual SWNTs.

The obtained theoretical results for individual SWNTs can qualitatively be extended to explain the experimental facts of magnetoresistance for MWNTs. But some unusual and interesting theoretical predictions, for example, that the exhibited AB effect is related to low-energy conducting electrons, and that the AAS effect is of a very small magnitude and difficult to observe, etc., remain to be verified through experimental measurements.

ACKNOWLEDGMENT

The work was financially supported by the Scientific Research Fund of Hunan Provincial Education Department (Grant No. 01C248).

*Corresponding author. Department of Information and Calculating Science, Changsha Communications College, Changsha 410076, The People's Republic of China. Email address: huazhenzhang@163.net

[1] S. J. Tans, M. H. Devoret, H. Dai, A. Thess, R. E. Smalley, L. J. Geerligs, and C. Dekker, Nature (London) **386**, 474 (1997).
[2] M. Bockrath, D. H. Cobden, P. L. McEuen, N. G. Chopra, A. Zettl, A. Thess, and R. E. Smalley, Science **275**, 1922 (1997).
[3] S. J. Tans, A. R. M. Verschueren, and C. Dekker, Nature (London) **393**, 49 (1998).
[4] K. Tsukagoshi, B. W. Alphenaar, and H. Ago, Nature (London) **401**, 572 (1999).
[5] P. G. Collins, A. Zettl, H. Bando, A. Thess, and R. E. Smalley, Science **278**, 100 (1997).
[6] M. S. Fuhrer, J. Nygard, L. Shih, N. Forero, Y.-G. Yoon, M. S. C. Mazzoni, H. J. Choi, J. Ihm, S. G. Louie, A. Zettl, and P. L. McEuen, Science **288**, 494 (2000).
[7] S. N. Song, X. K. Wang, R. P. Chang, and J. B. Ketterson, Phys. Rev. Lett. **72**, 697 (1994).
[8] L. Langer, V. Bayot, E. Grivei, and J.-P. Issi, Phys. Rev. Lett. **76**, 479 (1996).
[9] G. Baumgartner, M. Carrard, L. Zuppiroli, W. Bacsa, W. A. de Heer, and L. Forró, Phys. Rev. B **55**, 6704 (1997).
[10] G. T. Kim, E. S. Choi, D. C. Kim, D. S. Suh, Y. W. Park, K. Liu, G. Duesberg, and S. Roth, Phys. Rev. B **58**, 16 064 (1998).
[11] H. R. Shea and R. Martel, Phys. Rev. Lett. **84**, 4441 (2000).
[12] M. Baxendale, V. Z. Mordkovich, S. Yoshimura, and R. P. H. Chang, Phys. Rev. B **56**, 2161 (1997).
[13] G. Bergmann, Phys. Rep. **107**, 1 (1984).
[14] A. Bachtold, C. Strunk, J.-P. Salvetat, J. M. Bonard, L. Forró, T. Nussbaumer, and C. Schönenberger, Nature (London) **397**, 673 (1999).
[15] B. L. Altshulre, A. G. Aronov, and B. Z. Spivak, Pis'ma Zh. Eksp. Teor. Fiz. **33**, 101 (1981) [JETP Lett. **33**, 94 (1981)].
[16] A. Fujiwara and K. Tomiyama, Phys. Rev. B **60**, 13 492 (1999).
[17] Y. Aharonov and D. Bohm, Phys. Rev. **115**, 485 (1959).
[18] H. Ajiki and T. Ando, J. Phys. Soc. Jpn. **62**, 1255 (1993).
[19] M. F. Lin and K. W.-K. Shung, Phys. Rev. B **52**, 8423 (1995).
[20] J. P. Lu, Phys. Rev. Lett. **74**, 1123 (1995).
[21] A. Bezryardin, A. R. M. Verschuercn, S. J. Tans, and C. Dekker, Phys. Rev. Lett. **80**, 4036 (1998).

[22] M. R. Falvo, G. J. Clary, R. M. Taylor II, V. Chi, F. P. Brooks, Jr., S. Washburn, and R. Superfine, Nature (London) **389**, 582 (1997).
[23] C. Schönenberger, A. Bathtold, C. Trunk, J.-P. Salvetat, and L. Forró, Appl. Phys. A: Mater. Sci. Process. **69**, 283 (1999).
[24] A. G. Aronov and Y. V. Sharvin, Rev. Mod. Phys. **59**, 755 (1987).
[25] Z. Yao, C. L. Kane, and C. Dekker, Phys. Rev. Lett. **84**, 2941 (2000).
[26] Zhenhua Zhang, Jingcui Peng, and Hua Zhang, Appl. Phys. Lett. **79**, 3515 (2001).
[27] N. Byers and C. N. Yang, Phys. Rev. Lett. **7**, 46 (1961).
[28] R. Saito, G. Dresselhaus, and M. S. Dresslhaus, *Physical Properties of Carbon Nanotubes* (Imperial College Press, London, 1998), p. 37.
[29] R. A. Jishi, M. S. Dresslhaus, and G. Dresselhaus, Phys. Rev. B **47**, 16 671 (1993).
[30] Z. H. Zhang and J. C. Peng, Chin. J. Chem. Phys. **14**, 197 (2001).
[31] O. M. Yevtushenko, G. Ya. Slepyan, and S. A. Maksimenko, Phys. Rev. Lett. **79**, 1102 (1997).
[32] A. S. Maksimenko, G. Ya. Slepyan, and G. Y. Slepyan, Phys. Rev. Lett. **84**, 362 (2000).
[33] L. X. Benedict, V. H. Crespi, S. G. Louie, and M. L. Cohen, Phys. Rev. B **52**, 14 935 (1995).
[34] C. T. White and J. W. Mintmire, Nature (London) **394**, 29 (1998).